ISSN (Print) 1226-1750
ISSN (Online) 2233-6656
Journal of Magnetics 24(4), 739-743 (2019) https://doi.org/10.4283/JMAG.2019.24.4.739

A Feasibility Study of GAGG-GAPD Detector for Development of DEXA

Jingyu Yang[1], Byung Jun Min[3], and Jihoon Kang[1,2]*

[1]*Department of Biomedical Engineering, Chonnam National University, Yeosu 59626, Republic of Korea*
[2]*Research Center for Healthcare-Biomedical Engineering, Chonnam National University, Yeosu 59626, Republic of Korea*
[3]*Department of Radiation Oncology, Chungbuk National University Hospital, Cheongju 28644, Republic of Korea*

(Received 10 November 2019, Received in final form 4 December 2019, Accepted 9 December 2019)

A GAGG-GAPD detector module was proposed and developed for DEXA application and was characterized under various conditions. The proposed detector consists of GAGG and GAPD. The effect of kVp on energy spectra was assessed for different tube voltages in air condition. Also, the effect of the filter on dual energy X-ray spectra was examined by using K-edge filter with different thickness. The mean photon energy and beam peak energy are increase linearly from 40 kVp to 80 kVp. The dual energy peaks were located around 32 keV and 65 keV and were considerably isolated. The DEXA phantom image for each steps were clearly resolved. These results demonstrate the feasibility of GAGG-GAPD detector allowing more potential merits than conventional CZT detector for DEXA application.

Keywords : Dual-energy X-ray absorptiometry (DEXA), bone mineral density (BMD), Gadolinium Aluminum Gallium Garnet (GAGG), Geiger-mode avalanche photodiodes (GAPD)

1. Introduction

There has been considerable interest in measuring the bone mineral content and density. Magnetic resonance imaging (MRI) or computed tomography (CT) are the most accurate methods for measurement of body composition. However, they have some limitations such as high cost, long scan time, or high exposure from X-ray [1, 2]. Dual-energy X-ray absorptiometry (DEXA) is alternate method with low dose, cost-effective, and short scan time [2-4]. For minimizing problems of conventional DEXA detector based on semiconductor [5, 6], X-ray diagnostic detector consisted of scintillation crystals and photosensor have attracted interest for their use in DEXA applications. First commercial DEXA scanner using lutetium yttrium oxyorthosilicate (LYSO) and Geiger-mode avalanche photodiodes (GAPD) has recently been introduced [7].

Recently, Ce doped GAGG is a newly developed single-crystal scintillator which has relatively high density (6.63 g/cm^3), high light yield (46 photons/keV), and short decay time (~88 ns). Furthermore, its non-hydroscopic characteristic make the fabrication of scintillator blocks suited for radiation imaging modality. Compare with LSO/LYSO scintillator, GAGG does not contain natural radioactivity caused by ^{176}Lu, thus background count rates can be removed [8]. GAGG have been studied actively for the development of radiation detector and they were reported elsewhere [9-11].

The aim of this study was to develop and evaluate a DEXA detector based on GAGG scintillation crystal and GAPD photosensor. The intrinsic performance of the DEXA detector module was characterized under a variety of conditions. The initial results of phantom were presented to demonstrate the feasibility of dual-energy X-ray imaging with this prototype.

2. Materials and Methods

2.1. X-ray source module

The integrated monoblock system (XRB80 Monoblock; Spellman High Voltage Electronics Corp., USA) was used in this study. X-ray tube in a sealed tank has a fixed tungsten anode and a focal spot size of 0.5 mm. The maximum tube voltage and tube current are 80 kVp and 1.25 mA, respectively. The X-ray pass through a Ce sheet for absorbing X-ray photons around the K-shell energy (~40 keV) [12]. It could generate the effective energy

*Corresponding author: Tel: +82-61-659-7369
Fax: +82-61-659-7363, e-mail: ray.jihoon.kang@gmail.com

peaks of ~30 keV and ~60 keV. The K-edge filter module consists of seven Ce-sheet components of 0.1 mm thickness (Alfa Aesar, Ward Hill, USA), and the variable different filter thicknesses ranging from 0.1 mm to 0.7 mm permit the intensity of the X-ray beam to be optimized for patient thickness. The lead collimator with a 3 mm thickness was installed between the X-ray tube and K-edge Ce filter module to achieve pencil-beam collimation.

2.2. GAGG-GAPD detector

The gadolinium aluminum gallium garnet (GAGG) scintillation crystal was employed for the development of DEXA detector because it could provide excellent properties, such as fast decay time (~90 ns), high light output (~45 photons/keV) and low cost [9-11]. In addition, it has a good stopping power for the DEXA energy range in 20 keV to 100 keV. The thickness of GAGG was fixed to 3 mm for estimating detection efficiency of > 99.9 % for 80 keV, while conventional CZT should increase the thickness to 5 mm. The GAGG consisted of $3 \times 3 \times 3$ mm^3 crystal pixel and all surface were wrapped with teflon tape except for bottom surface coupling with photosensor. A Geiger-mode avalanche photodiodes (GAPD) (MicroFJ-SMPTA-30035; On Semiconductor, Arizona, USA) was used for the scintillation light readout. It has an active area of 3.07×3.07 mm^2 consisted of 5,676 microcells of the 35×35 μm^2 (Fig. 1).

2.3. Signal processing electronics

Output signals from GAGG-GAPD DEXA Detector were fed into custom-made current feedback charge-sensitive preamplifier using high gain operational amplifiers (AD8012; Analog Devices Inc, Norwood, USA). The amplifier circuit is consisted of amplifier, amplification adjustment potentiometer and feedback capacitor for reduce noise. The amplified signal was split into two signals. Signal was digitized and recorded by the custom-made data acquisition (DAQ) system based FPGA. The digitized outputs were converted to energy spectra for each interaction event.

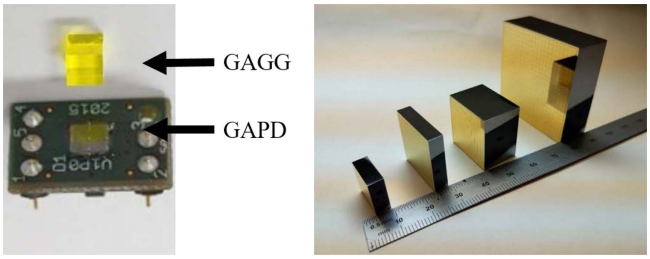

Fig. 1. (Color online) The proposed GAGG-GAPD detector (left) and conventional widely utilized CZT detector (right) for DEXA Application [6].

2.4. Estimation and measurement of spectral response

A simulation study was performed to generate the reference X-ray energy spectra by using the tungsten anode spectral model using interpolating polynomials (TASMIP) algorithm [13]. Different X-ray tube spectra in 1 keV bins was simulated for voltages between 40 and 80 kVp in 10 kVp intervals, and the beam peak energy and mean photon energy were calculated. A focus-to-detector distance was 750 mm.

The exposure measurements were performed at the same settings described above. The validation of X-ray spectra was performed by comparing simulated and measured results in air condition. The energy spectra were acquired for 10 sec for each tube voltage. The effect of kVp on energy spectra was assessed, by calculating the beam peak energy and mean photon energy values at 0.01 mA tube current and comparing with simulation results.

2.5. Effect of K-edge Ce filter on dual-energy discrimination

Seven different thickness of Ce filter ranging from 0.1 mm to 0.7 mm, with 0.1 mm steps were used to examine the effect of the K-edge filter on dual-energy spectra. The X-ray tube was operated at 80 kVp and 0.1 mA, and the filtered dual-energy spectra were acquired for 1 min. Counts per second (CPS) was characterized by the dual-energy X-ray spectra.

2.6. Image performance

The imaging capability of the GAGG-GAPD detector developed in this study was evaluated by using a bone mineral densities (BMDs) phantom simulated bone and soft tissue. The phantom consisted of acrylic and aluminum instead of soft tissue and bone mineral, respectively [14]. The thickness of acrylic and aluminum is 120 mm and 4, 6, 8, 10 and 12 mm, respectively. A K-edge Ce filter of 0.3 mm thickness was used for image performance and X-ray tube was operated at 80 kVp and 0.1 mA. The amount of counted photons were separated to low and high energy. These dual energy images were converted into density images by using conventional dual energy subtraction algorithm [12].

3. Results

3.1. Estimation and measurement of spectral response

The measured X-ray energy spectra as a function of tube voltage from 40 kVp to 80 kVp were similar in shape to the simulated one (Fig. 2). Fig. 3 shows the

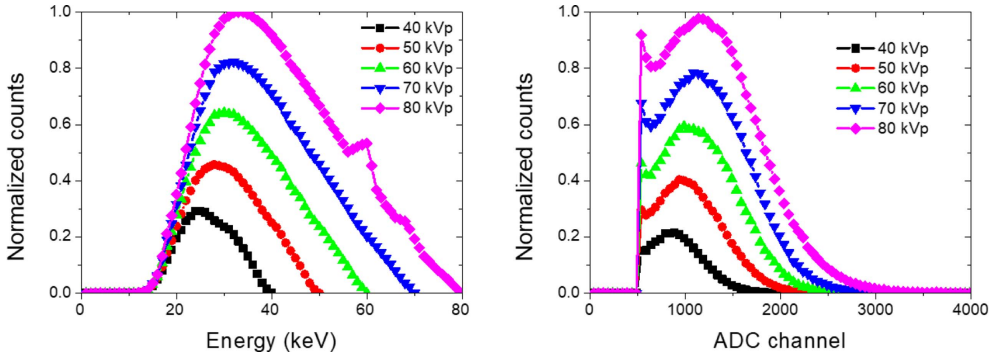

Fig. 2. (Color online) X-ray spectra as a function of tube voltage obtained from simulation (left) and experiment (right).

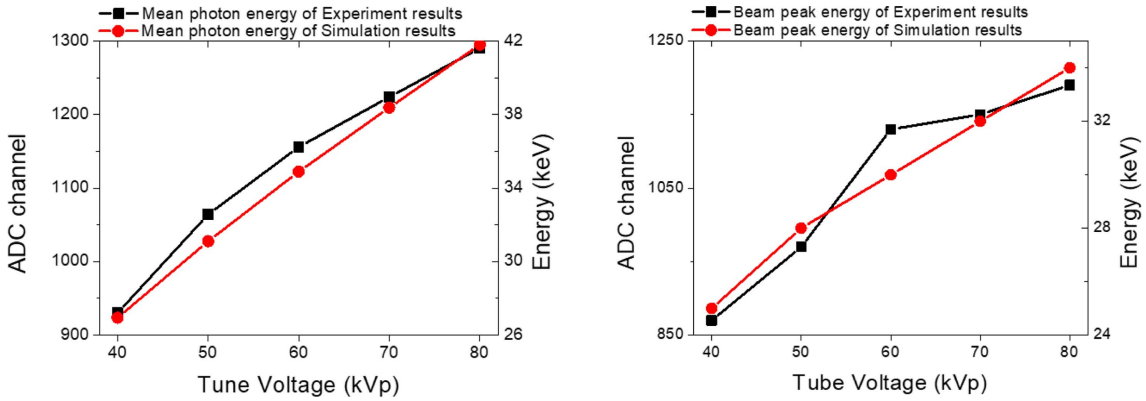

Fig. 3. (Color online) Mean energy photon (left) and beam peak energy (right) of experiment (square) and simulation (circle) results.

mean photon energy and beam peak energy of simulation and experiment results, respectively. The mean photon energy increase from 28.4 keV to 43.8 keV and from 929 to 1,289 ADC channel, and the beam peak energy increase from 28 keV to 36 keV and from 757 to 1,190 ADC channel for simulation and measurement, respectively.

3.2. Effect of K-edge Ce filter on dual-energy discrimination

Fig. 4 shows the dual-energy X-ray spectra for different thickness of K-edge Ce filter. The dual energy peaks were located around 32 keV and 65 keV and were isolated when thickness of Ce filter was 0.3 mm or over. The CPS

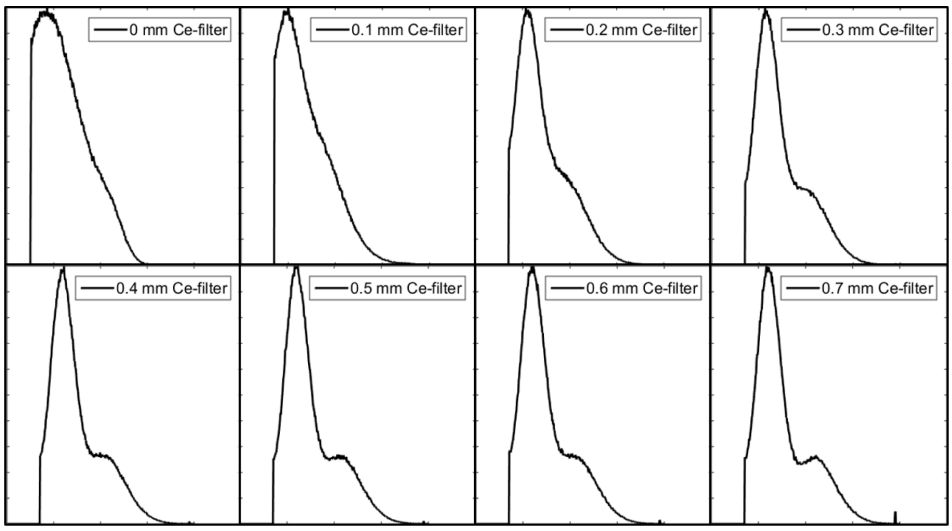

Fig. 4. X-ray energy spectrum as a function of K-edge Ce filter thickness.

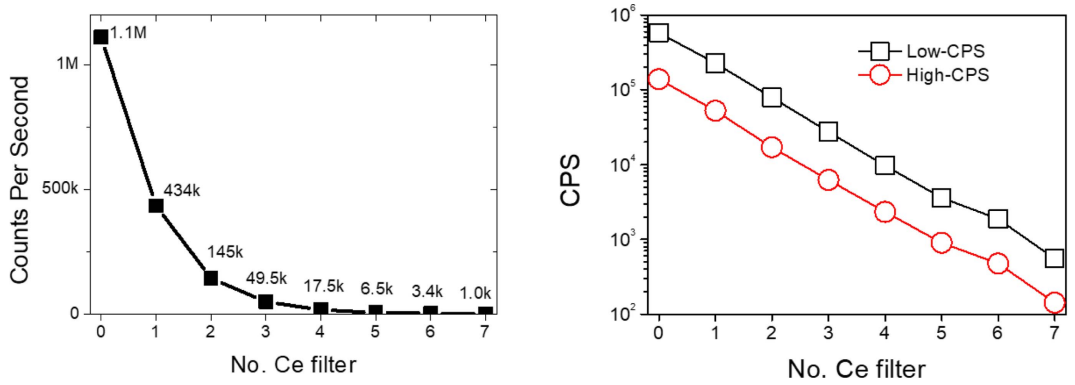

Fig. 5. (Color online) All (left), low- and high-CPS (right) as a function of K-edge Ce filter thickness.

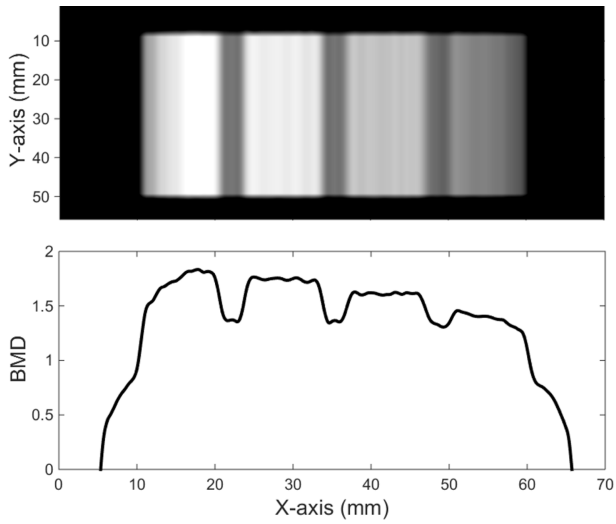

Fig. 6. Acquired DEXA Image (top) and line profile (bottom) by step phantom.

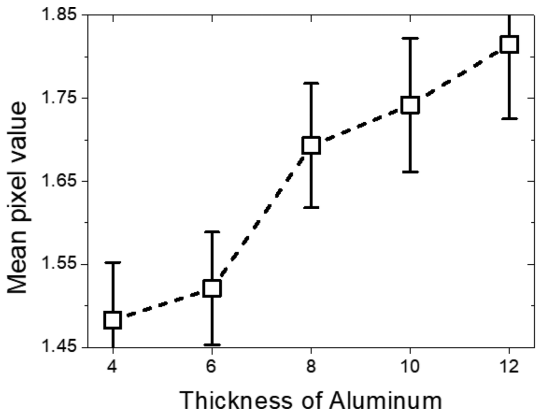

Fig. 7. Mean pixel value and standard deviation correspond to aluminum thickness from 4 mm to 12 mm (bottom).

was decreased from 434 kcps to 1 kcps as a function of K-edge Ce filter thickness. Also, CPS of low- and high-energy were exponentially decreased (Fig. 5).

3.3. Image performance

Fig. 6 presents the DEXA image and line profile acquired with the proposed detector and step phantom. The value of acrylic was distinguished from values of aluminum steps. Also each steps of aluminum with 4, 6, 8, 10 and 12 mm thickness were clearly identified. Fig. 7 shows the mean pixel value and standard deviation correspond to each aluminum steps of phantom. The mean pixel values were increased from 1.48 to 1.81 while thickness of aluminum from 4 mm to 12 mm.

4. Discussion and Conclusions

A GAGG-GAPD DEXA detector was developed and evaluated. Various X-ray energy spectra as functions of tube voltage in air condition were acquired by using simulation estimation and experimental measurement. The measured X-ray energy spectra were similar in shape to the simulated one. The mean photon energy and beam peak energy linearly changed as function of tube voltage. These results were similar to those estimated by the simulation study. For discriminating low- and high-energy, Ce filter that could generate energy peaks of ~30 keV and 60 keV was used for K-edge filter in this study. Effect of K-edge Ce filter on dual-energy discrimination was characterized. The dual energy peaks of ~30 keV and ~60 keV were clearly identified with Ce filter of ≥ 0.3 mm thickness. Initial phantom images without noticeable artifacts or distortions were successfully acquired. Each step was clearly identified for the encapsulated spine phantom. Image pixel values were linearly increased as a function of Al thickness in the phantom.

Alternative DEXA detector based on LSO/LYSO crystal coupled with GAPD photosensor has been introduced recently for replacement of conventional cadmium zinc telluride (CZT) or cadmium telluride (CdTe) [5, 6]. Also, they have been employed in conventional DEXA scanner

by swapping a direct version of CZT for the indirect version of this detector. However, it was well known that LSO/LYSO contains natural radioactivity, ^{176}Lu, that emits beta particles, and these unavoidable background radiations could affect the count rate performance and image quality for DEXA system. On the contrary, GAGG does not include ^{176}Lu component, and it would be advantages for reducing error of count rates [8].

Compared to conventional CZT or CdTe detector, the proposed design could provide several potential merits while overcoming inevitable technical issues such as fragile structure, irradiation damage over time, incomplete charge collection caused by charge trapping, and large dark current by increasing temperature [15, 16]. The GAGG could allow relatively high count rate owing to its fast decay time (~88 ns), small crystal volume (~3 mm thickness) due to its good stopping power [9-11].

This study has some limitations. First, the intrinsic energy resolution would be relatively poor compared to CZT or CdTe based DEXA detectors, which was caused by the indirect conversion mechanism for incident X-rays [17]. However, it was feasible to distinguish low- and high-energy from incident dual-energy X-ray by using ≥ 3 mm thickness Ce filter and there are no considerable problems in image. Second, voltage and current of X-ray unit used in this study were relatively moderate compared to recently available X-ray tube with high power (max. 100 kVp & 3 mA) used in commercial DEXA scanner. On the other hand, the intrinsic performance was well characterized and the feasibility of alternative DEXA scanner with GAGG-GAPD detector was observed to some extent. Nevertheless, further studies will be needed to characterize detector performance and acquire various phantom images under high power X-ray tube conditions.

Acknowledgements

This research was supported by Basic Science Research Program through the National Research Foundation of Korea (NRF) funded by the Ministry of Education (NRF-2018R1D1A3B07040759), and by a grant (NRF-2018R1A4A1025704) of the Basic Science Research Program through the National Research Foundation of Korea (NRF) funded by the Ministry of Science and ICT, Republic of Korea.

References

[1] D. A. Fields, A. M. Teague, K. R. Short, and S. D. Chernausek, Pediatr Obes **10**, 5 (2015).
[2] I. Fogelman and G. M. Blake, J. Nucl. Med. **41**, 12 (2000).
[3] J. F. Aloia, A. Vaswani, R. Ma, and E. Flaster, J. Nucl. Med. **36**, 8 (1995).
[4] G. M. Blake and I. Fogelman, Semin. Nucl. Med. **31**, 1 (2001).
[5] T. Tadayuki and S. Watanabe, IEEE Trans. Nucl. Sci. **48**, 4 (2001).
[6] https://www.kromek.com/cadmium-zinc-telluride-czt/
[7] GE Healthcare. GE Prodigy Advance spec sheet. (2015).
[8] S. Yamamoto, H. Horii, M. Hurutani, K. Matsumoto, and M. Senda, Ann. Nucl. Med. **19**, 2 (2005).
[9] J. Y. Yeom, S. Yamamoto, S. E. Derenzo, V. C. Spanoudaki, K. Kamada, T. Endo, and C. S. Levin, IEEE Trans. Nucl. Sci. **60**, 2 (2013).
[10] S. Yamamoto, J. Y. Yeom, K. Kamada, T. Endo, and C. S. Levin, IEEE Trans. Nucl. Sci. **60**, 6 (2013).
[11] S. J. Lee and C. H. Baek, J. Kor. Soc. Radiol. **12**, 7 (2018).
[12] G. M. Blake and I. Fogelman, Semin. Nucl. Med. **27**, 3 (1997).
[13] J. M. Boone and J. A. Seibert, Med. Phys. **24**, 11 (1997).
[14] C. H. Baek and D. Kim, Nucl. Inst. Meth. A **799** (2015).
[15] J. Knag, Y. Choi, K. J. Hong, W. Hu, J. H. Jung, Y. Huh, and B. Kim, JINST **6**, P02012 (2011).
[16] J. Knag, Y. Choi, K. J. Hong, J. H. Jung, W. Hu, Y. Huh, and H. Lim, Med. Phys. **37**, 11 (2010).
[17] T. Takahashi and S. Watanabe, IEEE Trans. Nucl. Sci. **48**, 4 (2001).